



Experimental Study on Direct Reduction of Laterite Nickel Ore Leaching Residue Pellets

F. Yang^{1,*}, CH. Pi¹, ZH. Q. Guo¹, K. Xu¹, and J.Y. He¹

<https://doi.org/10.64486/m.66.1.3>

¹ Wuhan University of Science and Technology, College of Resources and Environmental Engineering, Hubei Key Laboratory for Efficient Utilization and Agglomeration of Metallurgic Mineral Resources, Wuhan, China.

* Correspondence: yangfu@wust.edu.cn

Type of the Paper: Article

Received: December 4, 2025

Accepted: April 28, 2026

Abstract: Pellets were formed by adding carbon to laterite nickel ore leaching residue in the laboratory and then reduction roasting was carried out. The effects of reduction conditions such as the ratio of reducing agents, reduction temperature, and reduction time on the products of direct reduction iron (total iron content and iron recovery rate) were studied. The research results show that under the conditions of a reducing agent (coal powder) ratio of 16 %, a reduction temperature of 1200 °C, and a reduction time of 40 minutes, the total iron content of directly reduced iron is 93.10 %, and the iron recovery rate is 96 %.

Keywords: leaching residue of laterite nickel ore pellets; direct reduction; reducing agent ratio; reduction temperature; reduction time

1. Introduction

The leaching residue of laterite nickel ore denotes the solid by-product remaining after the acid leaching process applied to laterite nickel ore [1-2]. Laterite nickel ore is a nickel-bearing mineral resource predominantly found in tropical regions, including the Philippines and Indonesia [3]. The leaching of laterite nickel ore is commonly conducted via high-pressure acid leaching (HPAL), a process that selectively extracts nickel and cobalt under elevated temperature and pressure conditions, while leaving the majority of impurities including iron and aluminum in the solid residue. The chemical composition of laterite nickel ore leach residue is highly complex, dominated by iron (30–55) %, with significant concentrations of nickel, cobalt, chromium, silicon, and aluminum [4]. From an environmental standpoint, the valorization of laterite nickel ore leach residue is essential to enabling green, efficient, and sustainable exploitation of laterite nickel resources. Cao et al. investigated the feasibility of utilizing hydrometallurgically processed leaching residue containing 59.2 % iron as a sustainable feedstock for the synthesis of lithium iron phosphate (LiFePO₄) cathode material [5]. Qiao et al. designed a method to extract iron from laterite nickel ore leaching residue and recycle it into high-valuable iron phosphate products using only phosphoric acid and iron powder. A final high-purity FePO₄ (99.4 %) was obtained [6]. Lei et al. reported on the reduction roasting of leaching residues, high-grade pig iron powder was obtained [7-10]. Xu et al. conducted experimental investigations into the reduction roasting - reduction smelting of laterite nickel ore leaching residue, yielding an alloy suitable for partial substitution of conventional ferroalloy feedstocks in steelmaking and a slag phase amenable to utilization as an active mineral admixture in cement production [11]. Laboratory-scale experiments were conducted to evaluate the efficacy of hydrogen plasma smelting reduction for the treatment of leaching residue. A hydrogen plasma treatment duration of 180

s enabled the production of a metallic product from nickel leaching residue with a sulfur content below 0.1 % and a chromium content exceeding 3 % [12].

This approach mitigates land-use inefficiency associated with the stockpiling of industrial residues particularly acid leach residue, while also reducing ecological risks linked to deep-sea disposal. From a resource utilization perspective, laterite nickel ore leach residue contains substantial concentrations of valuable metals including nickel, cobalt, and iron offering significant potential for secondary resource recovery. [13-14]. In China, the comprehensive utilization of laterite nickel ore leach residue remains largely confined to laboratory-scale research. This study investigates an integrated process—comprising internal coal blending, pelletizing, reduction roasting with magnetization, and magnetic separation—to address land occupation, safety, environmental, and resource recovery challenges associated with leach residue management, thereby establishing a technical foundation for efficient iron recovery from this residue.

2. Materials and Methods

The raw materials used in this experimental study include laterite nickel ore leaching residue and coal powder. The chemical composition of the leaching residue is shown in Table 1. In this experiment, coal powder was used as a reducing agent to crush it and control its particle size to below 0.074 mm. It was then mixed with leaching residue to prepare pellets for reduction roasting. The industrial analysis results of coal powder are shown in Table 2.

Table 1. Chemical compositions of leaching residue

Components	Fe ₂ O ₃	SiO ₂	CaO	Al ₂ O ₃	Cr ₂ O ₃	MgO	MnO
Content /%	73.42	5.80	0.03	3.25	2.98	0.51	0.17

Table 2. Industrial analysis of coal powder /%

FC _d	A _d	V _d	Mad
72.92	12.11	11.85	3.12

In this study, different proportions of coal powder and leaching residue were mixed evenly for pelletizing. Based on the previous pelletizing experiments, the leaching residue has good pelletizing performance, so no binder such as bentonite needs to be added. The green pellets were dried and then were subjected to reduction roasting in a muffle furnace at different temperatures. Once the vacuum resistance furnace reached the target temperature, the pellet-loaded crucible was sealed and introduced into the furnace for reduction roasting. Upon completion of the reduction roasting period, the crucible was allowed to cool inside the furnace.

After cooling, the reduced roasting slag was subjected to low-intensity magnetic separation using a magnetic separator operated at a magnetic field strength of 160 kA/m, with tap water serving as the separation medium. The resulting magnetic concentrate was subsequently vacuum-filtered and dried. Its chemical composition was quantified by inductively coupled plasma optical emission spectrometry (ICP-OES), and the iron recovery rate (η) was calculated according to equation (1). The effects of reduction conditions such as the ratio of reducing agent, reduction temperature and reduction time on the direct reduced iron product (total iron content and iron recovery rate of reduced iron) were investigated.

$$\eta = \frac{w_1 \times m_1}{w_2 \times m_2} \times 100\% \quad (1)$$

where:

w_1 , w_2 - respectively the mass fractions of Fe in the magnetic separation concentrate and the original leaching residue/%,

m_1 , m_2 - the corresponding total masses of the magnetic concentrate and the original leaching residue/g.

3. Results and Discussion

Under the experimental conditions of a reduction temperature of 1200 °C and a reduction time of 1 hour, the effect of the ratio of reducing agents on the total iron content and iron recovery rate of direct reduced iron was systematically examined. The results are presented in Figure 1.

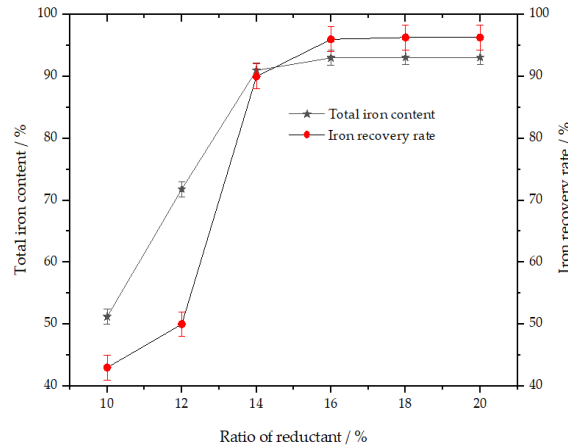


Figure 1. The effect of reducing agent ratio on the total iron content and iron recovery rate of directly reduced iron

As shown in Figure 1, when the coal powder ratio is less than 16 %, as the coal powder ratio increases, the total iron content and iron recovery rate of direct reduced iron also increase. When the coal powder ratio exceeds 16 %, the total iron content and iron recovery rate of direct reduced iron remain almost unchanged. It is explained that when the ratio of the reducing agent is insufficient, the reduction reaction of iron oxides is not complete, resulting in low total iron content and iron recovery rate. Therefore, the ratio of the reducing agent is determined to be 16 %. At this point, the total iron content of direct reduced iron is 93 % and the iron recovery rate is 96 %.

Under the conditions of a 16 % concentration of the reducing agent and a reduction time of 1 hour, experiments were conducted to investigate the influence of the reduction temperature on the total iron content and iron recovery rate of direct reduced iron. The results are shown in Figure 2.

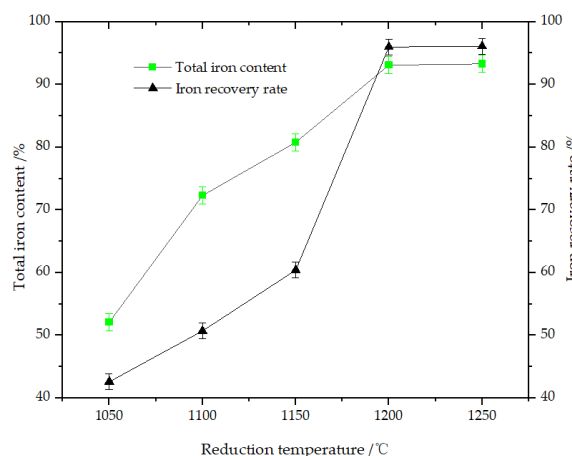


Figure 2. The effect of reduction temperature on the total iron content and iron recovery rate of directly reduced iron

As illustrated in Figure 2, when the reduction temperature is 1050 °C, the total iron content is only 52.10 %. With increasing temperature, the Boudouard reaction intensifies, leading to a higher concentration of the reducing atmosphere within the pellet [15-16]. Consequently, the rate of elemental iron formation accelerates, and the total iron content continues to rise, reaching a maximum at 1200 °C, after which it stabilizes. Therefore,

the experimental reduction temperature is set at 1200 °C. At this temperature, the total iron content of direct reduced iron is 93.10 %, with an iron recovery rate of 96 %.

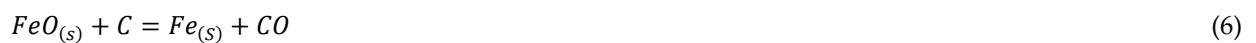
When the temperature exceeds 570 °C, the reduction of iron oxides proceeds stepwise, the reduction process is as follows.



$$\Delta_r G_m^\theta = 12000 - 218.46T \quad \text{J/mol} \tag{3}$$



$$\Delta_r G_m^\theta = 207510 - 217.62T \quad \text{J/mol} \tag{5}$$



$$\Delta_r G_m^\theta = 158970 - 160.25T \quad \text{J/mol} \tag{7}$$

Direct reduction of iron oxides using carbon as the reductant is thermodynamically and kinetically hindered, primarily due to the absence of effective solid–solid interfacial contact between the oxide phase and elemental carbon. Instead, under high-temperature conditions, elemental carbon undergoes the Boudouard reaction to generate carbon monoxide, which acts as the predominant gaseous reducing agent for iron oxide reduction.



$$\Delta_r G_m^\theta = 1707 - 174.47T \tag{9}$$

For instance, the direct reduction of wüstite (FeO) serves as a representative case. The equation representing the indirect reduction of wüstite (FeO) is given below.



$$\Delta_r G_m^\theta = -22800 + 24.26T \tag{11}$$

Equation (6) is obtained by algebraic combination of equations (8) and (10). The Boudouard reaction proceeds to near-completion only above approximately 1000 °C. An effective way to achieve a stronger reducing atmosphere is to moderately increase the temperature under the premise that the system pressure is not too high [17-18]. In the present experimental study, heat losses necessitated operation at an elevated temperature of 1200 °C to ensure sufficient driving force for complete reduction.

Under the conditions of a reduction temperature of 1200 °C and a reduction agent ratio of 16 %, experiments were conducted to investigate the influence of reduction time on the total iron content and iron recovery rate of directly reduced iron. The results are shown in Figure 3.

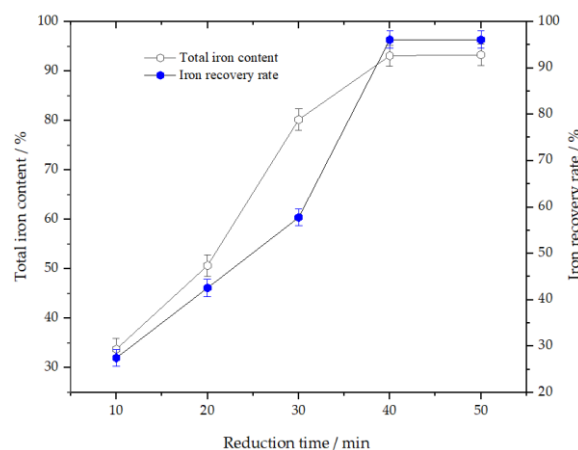


Figure 3. The effect of reduction time on the total iron content and iron recovery rate of directly reduced iron

From Figure 3, it can be seen that as the reduction time increases, the degree of direct reduction of iron oxides deepens, the total iron content increases, reaches a maximum value, and finally tends to flatten to a relatively stable state. When time is limited, the primary reaction is the formation of FeO, leading to an incomplete conversion of iron oxide to iron, which results in a lower grade of directly reduced iron products. As time progresses, the reduction of FeO to Fe becomes more thorough, with an increase in the amount of elemental iron produced. This elevates the grade of directly reduced iron to a certain level before stabilizing. Since solid carbon gasification and the reduction of ferrous oxide to metallic iron are the rate-limiting steps in the reaction, the reducing atmosphere created by solid carbon gasification accelerates the reduction rate of iron oxide. When the experimental duration reaches 40 minutes, both the solid carbon gasification and iron oxide reduction processes tend towards completion, and the total iron content gradually stabilizes. Consequently, the experimental reduction time was set at 40 minutes, at which point the total iron content of the directly reduced iron was 93.10 %, with an iron recovery rate of 96 %.

Direct reduction experiments were conducted on pellets of laterite nickel leaching residue under the conditions of 16 % pulverized coal ratio, a reduction temperature of 1200°C, and a reduction time of 40 minutes. The Figure 4 is the photo of reduced pellets.



Figure 4. The photo of reduced laterite nickel ore leaching residue pellets

As can be seen from Figure 4, the reduced pellets are loose, porous and have a metallic luster.

The reduced pellets shown in Figure 4 were crushed, subjected to magnetic separation, and subsequently processed to yield high-purity iron powder. The microscopic morphology of high-purity iron powder was observed and analyzed using the conductive adhesive bonding method, and its chemical composition was analyzed by means of energy dispersive spectrometer (EDS). The results are shown in Figure 5.

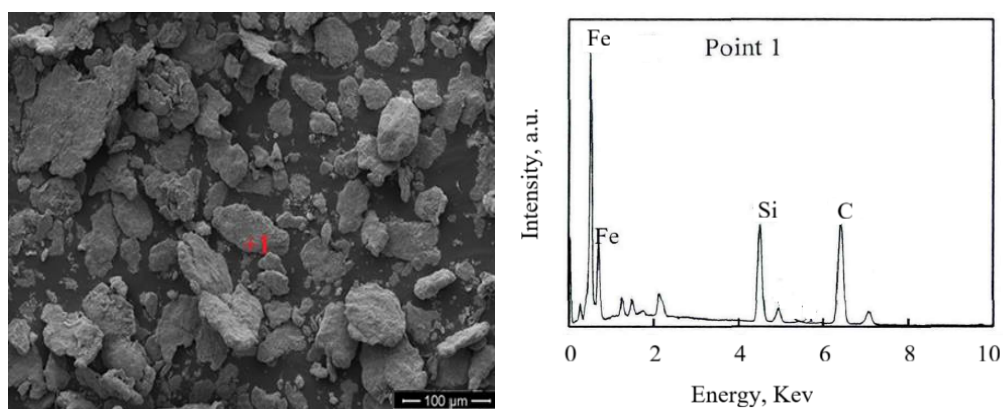


Figure 5. SEM and EDS analysis of high-purity iron powder

The SEM image shows that the high-purity iron powder is in the form of flakes and cakes. This is mainly due to the ductility of iron, which is caused by the compression during the crushing process of the elemental

iron. At the same time, it proves that the iron grains grow well and the grains are relatively large. According to EDS analysis, high-purity iron powder also contains other elements such as carbon.

The primary components of the directly reduced iron are listed in Table 3.

Table 3. The main component of direct reduced iron /%

Components	TFe	MFe	S	P	C	Si	Mn
Content	93.10	90.15	0.02	0.15	0.56	0.57	0.32

As can be seen from Table 3, the carbon content in direct reduced iron reaches 0.56 %, which is relatively high. This is due to the carburizing reaction that occurs during the reduction process. Because the activity of reduced iron is high, it can promote the decomposition of adsorbed CO, and the released C is absorbed by the iron, thereby forming Fe₃C [19-20]. In the low-temperature region, the reduced Fe is in a solid porous state, called sponge iron. The mechanism of the carburizing reaction is as follows.

Due to the ease of the equation (12) reaction at low temperatures, carbon black is precipitated.



The newly formed Fe has a catalytic effect on the above carbon precipitation reaction. The carbon infiltration reaction in sponge iron is described by equation (13).



5. Conclusions

Under the optimized reduction conditions—namely, a coal powder dosage of 16 %, a reduction temperature of 1200 °C, and a reduction duration of 40 min—the direct reduced iron (DRI) achieves a total iron content of 93.10 % and an iron recovery rate of 96 %.

The elevated carbon content in the DRI arises from carburization of metallic iron during reduction, driven by carbon diffusion from the solid reductant into the nascent iron phase.

References

- [1] L. Dan, "Research Progress and Application Prospect of Hydrometallurgy for Low Grade Laterite Nickel Ore," *Hydrometallurgy of China*, Vol.43, no.4, pp. 345-356, 2024. (In Chinese).
- [2] G.L. Xu, X. F. Xu, CH. Li, et al., "Research Progress on Resource Utilization of Leaching Residue of Laterite Nickel Ore," *China Nonferrous Metallurgy*, Vol.54, no.4, pp. 1-10, 2025. (In Chinese). <https://doi.org/10.19612/j.cnki.cn11-5066/tf.2025.04.001>
- [3] Q. Xu, W. CH. Xue, S. Y. Xu, et al., "Generation of Laterite-nickel Resources and Their Prospecting and Exploration in Indonesia," *Mineral Resources and Geology*, Vol.23, no.1, pp. 73-75, 2009. (In Chinese). <https://doi.org/10.3969/j.issn.1001-5663.2009.01.015>
- [4] L. F. Luo, Z. W. Li, and Z.G. Zhong, "Experimental Study on Iron Recovery from Leaching Residue of Lateritic Nickel Ore," *Mining and Metallurgical Engineering*, Vol.43, no.5, pp. 47-49+53, 2023. (In Chinese). <https://doi.org/10.3969/j.issn.0253-6099.2023.05.010>
- [5] Z. Cao, B. Ma, Q. Jing, et al., "Facile and Inexpensive Preparation Method of Iron Phosphate from Laterite Residue," *Ceram Int*, no.46, pp. 11304–11310, 2020, <https://doi.org/10.1016/j.ceramint.2020.01.159>
- [6] Y. CH. Qiao, H. M. Wang, CH. Liu, et al., "Recovery of High-Quality Iron Phosphate from Acid-Leaching Tailings of Laterite Nickel Ore," *Separation and Purification Technology*, Vol.353, pp. 1-7, 2025, <https://doi.org/10.1016/j.seppur.2024.128634>
- [7] M. G. Lei, B. Ma, Y. Chen, et al., "Effective Separation and Beneficiation of Iron and Chromium from Laterite Sulphuric Acid Leach Residue," *ACS Sustainable Chem Eng*, no. 8, pp. 3959–3968, 2020,

- <https://doi.org/10.1021/acssuschemeng.0c00219>
- [8] Z. Bai, Z. Wu, S. Yuan, et al., "Magnetic Separation for Recovering Iron Resources from Acid-Leaching Tailings of Laterite Nickel Ore through Mineral Phase Transformation," *Separation and Purification Technology*, Vol. 342, no.21, pp. 1-10, 2024, <https://doi.org/10.1016/j.seppur.2024.126931>
- [9] M. J. Rao, G. H. Li, X. Zhang, et al., "Reductive Roasting of Nickel Laterite Ore with Sodium Sulphate for Fe-Ni Production. Part II: Phase Transformation and Grain Growth," *Separation Science and Technology*, Vol.51, no.10, pp. 1727-1735, 2016, <https://doi.org/10.1080/01496395.2016.1166134>
- [10] X. Y. Guo, Q. Q. Gong, W. T. Shi, et al., "Magnetic Roasting of Pressure Leaching Residue of Nickel Laterite a Weak Magnetic Separation of Iron Concentrate," *Journal of Central South University (Science and Technology)*, Vol.43, no.6, pp. 2048-2053, 2012. (In Chinese).
- [11] G. L. Xu, X. F. Xu, CH. Li, et al., "Experimental Study on Reduction Roasting-Reduction Smelting of Leaching Residue of Laterite Nickel Ore," *Sustainable Mining and Metallurgy*, Vol.41, no.3, pp. 6-13, 2025. (In Chinese).
- [12] Zulfiadi Zulhan, Baihaqi Hakim, Yopi Hendrawan, et al., "Rapid Iron Extraction from Nickel Leaching Residue by a Hydrogen Plasma Smelting Reduction," *Journal of Materials Research and Technology*, Vol.30, pp. 5346-5355, 2024, <https://doi.org/10.1016/j.jmrt.2024.04.205>
- [13] R. Jiang, X. D. Guo, "Experimental Study on the Recovery of Iron Minerals from Acid Leaching Slag of Laterite Nickel Ore," *Gansu Metallurgy*, Vol.30, no.4, pp. 15-18, 2008. (In Chinese). <https://doi.org/10.3969/j.issn.1672-4461.2008.04.006>
- [14] M. Q. Dong, W. Chen, and Y. K. Zhu, "Development and Utilization of Iron Resources in Laterite Nickel Mine: a Review," *Mining and Metallurgy*, Vol.32, no.2, pp. 107-112, 2023. (In Chinese). <https://doi.org/10.3969/j.issn.1005-7854.2023.02.014>
- [15] T. Coetsee, P. C. Pistorius, E. Villiers, "Rate-determining Steps for Reduction in Magnetite-coal Pellets," *Minerals Engineering*, Vol.15, no.11, pp. 919-929, 2002, [https://doi.org/10.1016/s0892-6875\(02\)00120-6](https://doi.org/10.1016/s0892-6875(02)00120-6)
- [16] X. Y. Ning, G.Q. Xue, G. Wang, et al., "Mechanism of Direct Reduction and Melting-Separation for Carbon-bearing Pellets," *Chinese Journal of Engineering*, Vol.36, no.9, pp. 1166-1173, 2014. (In Chinese). <http://cje.ustb.edu.cn/article/doi/10.13374/j.issn1001-053x.2014.09.006>
- [17] C. L. Wang, H. F. Yang, B.P. Jiang, et al., "Experiments on Direct Reduction-Low Intensity Magnetic Separation of a Limonite in Yunnan Province," *Metal Mine*, Vol.43, no.5, pp. 74-77, 2014. (In Chinese).
- [18] J. Fang, W. X. Juan, *Non-Blast Furnace Ironmaking Processes and Theories*, Beijing: Metallurgical Industry Press, 2010. (In Chinese).
- [19] Y. A. Hui, D.Y. Wang, and M. F. Jiang, "Phase Analysis and Production Mechanism of Iron Carbide," *Journal of Northeastern University (Natural Science)*, Vol.24, no.9, pp. 828-831, 2003. (In Chinese). <https://doi.org/10.3321/j.issn:1005-3026.2003.09.004>
- [20] Y. J. Liang, Y. C. Che, *Manual of Abio-Therm-Odynamics*, Shenyang: Northeastern University Press, 1993. (In Chinese).